Evaluation of a Perturbative Retrieval Technique for Temperature Profiling in the Lower Troposphere Using Differential Absorption Lidar (DIAL)

Owen Cruikshank[1,2], Luke Colberg[1], Kevin S. Repasky[1], Robert A. Stillwell[3], and Scott M. Spuler[3]
[1] Montana State University, Bozeman, MT 59717
[2] University of Wyoming, Laramie, WY 82071
[3] National Science Foundation National Center for Atmospheric Research, Boulder, CO 80301

Introduction

In response to a community-identified need for ground-based thermodynamic profiling of the troposphere, researchers at Montana State University (MSU), in collaboration with researchers at the National Science Foundation National Center for Atmospheric Research (NSF NCAR), have developed diode-laser-based micropulse DIAL (MPD) instruments, that provide humidity, aerosol, and temperature profiling capabilities.

This presentation discusses the accuracy of temperature retrievals using a perturbative technique, which combines a DIAL measurement of a temperature-sensitive oxygen (O_2) absorption line with a high spectral resolution lidar (HSRL) measurement of the aerosol backscatter profile near 770 nm. The laboratory-based lidar instrument was operated over a six-month period between April 21, 2022, and September 22, 2022. During this time, 40 radiosondes were launched, providing reference data to validate the accuracy of the DIAL-based temperature profiles.

The results indicate that DIAL-based temperature retrievals are within ±2.5 ºC between 0.4 km and 3 km (3.5 km) range during daytime (nighttime) operation, using a 300-meter range resolution and a 60-minute time resolution.

Instrument

The instrument uses two continuous-wave distributed Bragg reflector (DBR) diode lasers operating near 770 nm and a series of pulsed electro-optical switches to injection-seed a booster optical amplifier (BOA) with pulses of online and offline laser light. The BOA output is used to injection-seed a pulsed tapered semiconductor optical amplifier (TSOA), generating the lidar pulse train. After the TSOA, a matched axicon pair creates an annular beam that is coupled to the inner half of a 40-cm diameter telescope.

Light collected by the outer half of the telescope is directed into the optical receiver. This light, along with light collected by a 4-cm diameter, wide field of view telescope, passes through two narrow-band optical filters and an etalon for spectral filtering. The light is then split. One portion is detected by a fiber-coupled single-photon-counting avalanche photodiode (APD), while the other portion passes through a potassium atomic vapor cell before being detected by a second APD.

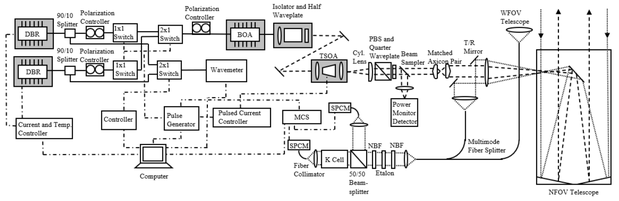


Figure 1: Schematic of the prototype MSU O2-DIAL and HSRL, comprising the temperature DIAL and HSRL. Acronyms: DBR – Distributed Bragg Reflector, BOA – Booster Optical Amplifier, TSOA – Tapered Semiconductor Optical Amplifier, PBS – Polarizing Beamsplitter, T/R – Transmit/Receive, NFOV – Narrow Field of View, WFOV – Wide Field of View, NBF – Narrow-Band Filter, K – Potassium, SPCM – Single-Photon-Counting Module, MCS – Multichannel Scaler.

Using the offline wavelength and the returns collected by the two channels of the optical receiver, an HSRL measurement provides the aerosol backscatter profile. Meanwhile, the channel without the potassium atomic vapor cell enables a DIAL measurement of the temperature-sensitive oxygen absorption coefficient using both the online and offline wavelengths.

This work focuses on the temperature retrieval and used a prototype instrument, shown in Figure 2, containing temperature and aerosol profiling capabilities. It should be noted that the temperature DIAL and HSRL can be combined with a water vapor DIAL for complete thermodynamic profiling in a single lidar instrument. A description of the complete thermodynamic profiler can be found in Stillwell et al. (2020).

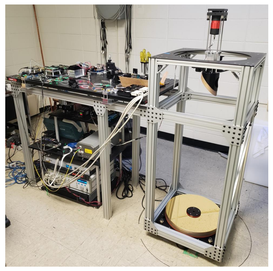


Figure 2: The MSU O_2-DIAL and HSRL.

Transmitter	
Wavelength	769.7958 nm (online) 770.1085 nm (offline)
Output Power	30 mW (combined)
Linewidth	< 2 MHz
Locking Tolerance	5 x 10^{-5} nm
Spectral Purity	99.90%
Repetition Rate	7 or 8 kHz (combined)
Receiver	
Etalon Finesse	15.43
Etalon FSR	157.90 GHz
NBF Bandwidth	0.75 nm
NBF Transmission	90%
Potassium Cell Length	72 mm
Potassium Cell Temperature	378 K

Table 1: Instrument parameters.

Temperature Retrieval

Previous work by Theopold and Bösenberg (1993) showed that DIAL temperature retrievals are possible using a temperature-sensitive oxygen absorption feature. However, they demonstrated that large errors of up to 10 ºC can occur if the lineshape of the backscattered signal is not considered. To address this issue, a DIAL temperature retrieval has been developed that incorporates an HSRL measurement of the backscatter ratio.

This temperature retrieval is a two-step process that incorporates a perturbative solution to the lidar equation to retrieve the oxygen absorption coefficient profile and an iterative retrieval to find the temperature profile from the retrieved absorption coefficient profile. Details of this retrieval technique can be found in Bunn et al. (2018) and Repasky et al. (2019).

The figure below shows the standard DIAL retrieval as α_{0th} and the perturbative correction terms α_{1st} and α_{2nd} that use the backscatter ratio to account for molecular broadening. The total oxygen absorption and the backscatter ratio are also shown for reference.

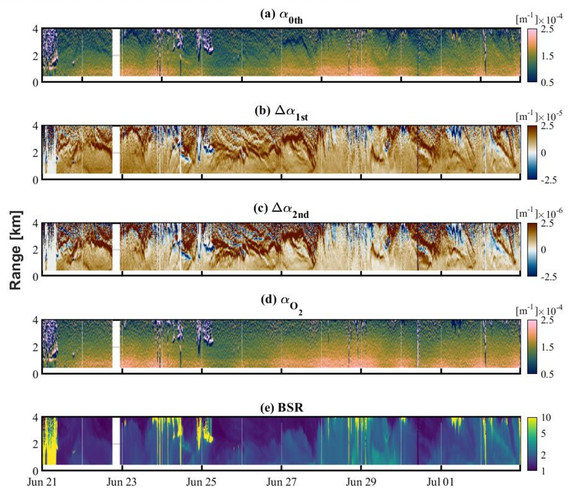


Figure 3: MSU O2-DIAL and HSRL data showing the effect of the backscatter ratio on the O_2 absorption and the perturbative correction. (a) Zero-order O_2 absorption coefficient, (b) first-order correction, (c) second-order correction, (d) total observed O_2 absorption coefficient, and (e) backscatter ratio. Note the changes in color and scale from Panels A-D. Temporal resolution of data in this figure is 10 minutes and range resolution is 75 meters. Time ticks are located at 00:00 UTC.

The iterative temperature retrieval utilizes the retrieved oxygen absorption coefficient and the known temperature and pressure dependence of the absorption linestrength and lineshape to retrieve the temperature profile. The oxygen absorption coefficient as a function of wavelength is shown in Figure 4. Care must be taken to account for all the relevant absorption lines near the MPD operating wavelengths. Details of the iterative temperature retrieval can be found in Repasky et al. (2019) and Cruikshank et al. (2024).

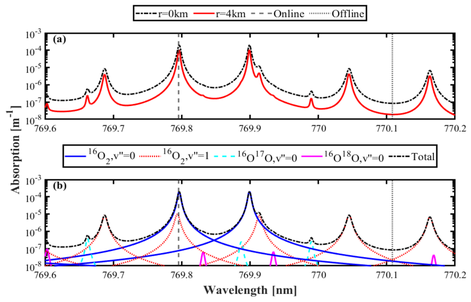


Figure 4: a) O_2 absorption spectrum in the wavelength region of interest. The model is shown at sea level and at a range of 4 km above mean sea level (assuming the 1976 US Standard Atmosphere). (b) The total O_2 absorption spectrum as the bold blue line, and each individual absorption line in the region of interest at the surface. Dashed vertical lines represent the online and offline DIAL wavelengths. All wavelengths are in vacuum. This figure shows how the absorption changes with altitude and the many separate absorption lines contributing to total absorption.

Acknowledgments

This material is based upon work supported by the Observations Program within the NOAA/OAR Office of Weather and Air Quality under award numbers NA19OAR4590323 and NA19OAR4590324.

This work was supported by the National Science Foundation under grant numbers 1917851 and 2234047.

Observational Data

The MPD instrument was operated between April 21, 2022, and September 22, 2022. Between April 21 and July 16, a pulse duration of 1 µs and a pulse repetition rate of 7 kHz were used. Between July 26 and September 22, a pulse duration of 750 ns and a pulse repetition rate of 8 kHz were used. The pulse length was changed in an attempt to address a consistent low-altitude bias, and the repetition rate was increased to account for the total pulse power loss.

A collocated radiosonde station was used to launch a total of 40 radiosondes over the course of the lidar operation, with 30 launched between April 21 and July 16 and 10 launched between July 26 and September 22. Radiosondes were launched at various times to sample a variety of daytime and nighttime conditions. Some days have multiple radiosonde launches to track the evolution of the planetary boundary layer height for a separate study. The retrieved temperature as a function of range and time is shown in Figure 5 and Figure 6. Radiosonde comparisons are shown in Figure 7 and Figure 8.

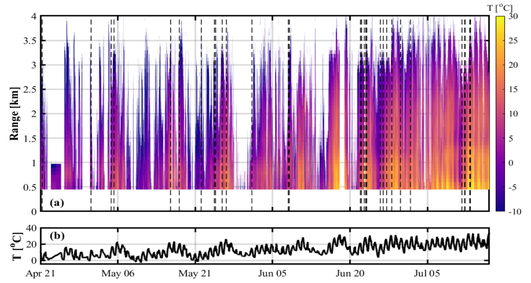


Figure 5: Temperature retrieval from the MSU O_2-DIAL and HSRL in the summer of 2022. Vertical dashed lines represent radiosonde launches. Areas in white represent a data mask. The data mask is from data availability, clouds, and low signal-to-noise ratio. Time ticks are located at 00:00 UTC. This figure shows the lidar range and performance over many weeks of operation, including the diurnal cycle. A pulse duration of 1 µs and a pulse repetition rate of 7 kHz were used. The line plot in the above figure shows the corresponding surface temperature measured using a collocated weather station.

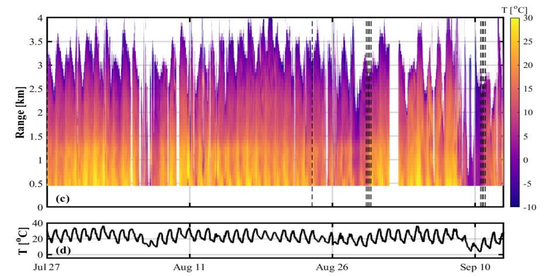


Figure 6: Same as above, using a pulse duration of 750 ns and a pulse repetition rate of 8 kHz.

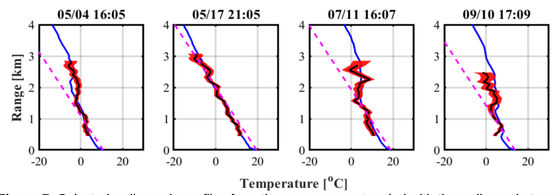


Figure 7: Selected radiosonde profiles from the measurement period with the radiosonde temperature in blue, DIAL temperature in black, and error colored in light red shading. The dry adiabatic lapse rate (-9.8 ºC/km) is shown as the dashed line. The individual performance of the DIAL temperature retrieval is shown compared to direct radiosonde measurements. Time and date are given in UTC.

References

Bunn, C. E., K. S. Repasky, M. Hayman, R. A. Stillwell, and S. M. Spuler, "Perturbative solution to the two-component atmosphere DIAL equation for improving the accuracy of the retrieved absorption coefficient," Appl. Optics, 57(16), 4440 (2018). doi:10.1364/ao.57.004440

Cruikshank, O., L. Colberg, K. S. Repasky, R. A. Stillwell, and S. M. Spuler, "Advancement and demonstration of a perturbative retrieval technique for temperature profiling in the lower troposphere using differential absorption light detection and ranging," J. Appl. Remote Sens., 18(3), 034514 (2024). doi:10.1117/1.JRS.18.034514

Repasky, K. S., C. E. Bunn, M. Hayman, R. A. Stillwell, and S. M. Spuler, "Modeling the performance of a diode laser-based (DLB) micro-pulse differential absorption lidar (MPD) for temperature profiling in the lower troposphere," Opt. Express, 27(23), 33543 (2019). doi:10.1364/OE.27.033543

Stillwell, R. A., S. M. Spuler, M. Hayman, K. S. Repasky, and C. E. Bunn, "Demonstration of a combined differential absorption and high spectral resolution lidar for profiling atmospheric temperature," Opt. Express, 28(1), 71 (2020). doi:10.1364/OE.379804

Theopold, F. A., and J. Bösenberg, "Differential absorption lidar measurements of atmospheric temperature profiles: theory and experiment," J. Atmos. Ocean. Tech., 10(2), 165–179 (1993). doi:10.1175/1520-0426(1993)010<0165:DALMOA>2.0.CO;2

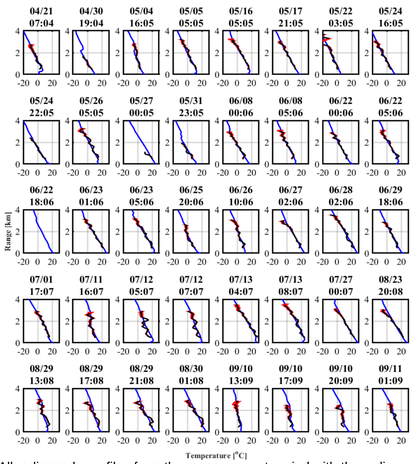


Figure 8: All radiosonde profiles from the measurement period with the radiosonde temperature in blue, DIAL temperature in black, and error colored in light red shading. Time and date are given in UTC.

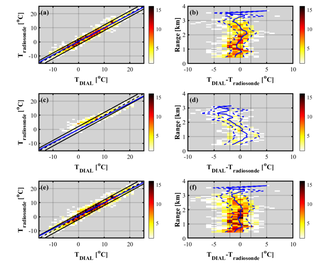


Figure 9: (a,c,e) Comparisons of radiosondes and DIAL temperature on 1:1 plots. The blue lines are linear fits, the black dashed lines are the 1:1 lines, and the black solid lines are ±2 ºC bounds. (a) Early summer with a 1-µs pulse length, (c) late summer with a 750-ns pulse length, and (e) combined summer comparison. (b, d, f) Corresponding comparisons of radiosonde and DIAL temperature profiles.

A comparison of the radiosonde temperature to the DIAL-retrieved temperature is shown in Figure 9. Using a linear fit to the scatter plots, the slope, fit, and correlation coefficients (R^2) were determined for three cases. In Figure 9a (early-summer, 1-µs pulse length), the slope is 0.966, the intercept is 0.3144 ºC, and R^2 is 0.956. For Figure 9c (late summer, 750-ns pulse length), the slope is 0.939, the intercept is -0.103 ºC, and R^2 is 0.945. In Figure 9e (combined comparison), the slope is 0.938, the intercept is 0.6479 ºC, and R^2 is 0.944.

Difference comparisons between radiosonde and lidar temperature as a function of altitude show a consistent bias that swings from positive to negative near 1 km above ground level. This is also seen in time series plots as horizontal banding, as shown in Figure 3. Slight horizontal banding can also be observed in water vapor MPD measurements, suggesting the bias stems from an issue with the MPD hardware architecture, perhaps involving the extended overlap function and pulse length. Different instruments and small differences in the alignment of the MPD show different shapes and amplitudes of the bias. In the observational period presented here, the pulse length of the lidar transmitter was changed from 1 µs to 750 ns in an attempt to reduce or change the bias. Figures 8b and 8d show the bias change between a 1-µs and a 750-ns pulse length. This effect is currently under investigation.

Each comparison bin has dimensions of 75 m and 10 minutes. Figures 8a and 8b have 979 bins for comparison, and Figures 8c and 8d have 325 bins. For the 1 µs pulse duration, the standard deviation is 1.76 °C with a mean error of -0.159 °C. For the 750 ns pulse duration, the standard deviation is 2.36 °C and a mean error of -0.784 °C. The combined data comparison has a standard deviation of 1.95 °C with a mean of -0.315 °C. Based on these results, the error in the temperature retrieval is approximately ±2.5 °C.

Summary

This work demonstrates the viability of the temperature-profiling micropulse DIAL to meet resolution and error recommendations for tropospheric measurements. Future advances in hardware and signal processing are expected to reduce bias and noise errors further. Combining temperature profiling with water vapor measurements enables retrievals such as virtual potential temperature and relative humidity, which could enhance the performance of numerical weather prediction models.